Published in final edited form as:
European J Org Chem. 2015 January 1; 2015(1): 109–121. doi:10.1002/ejoc.201402984.

Biosynthetically Distinct Cytotoxic Polyketides from *Setophoma terrestris*

Tamam El-Elimat[a], **Mario Figueroa**[b], **Huzefa A. Raja**[a], **Tyler N. Graf**[a], **Steven M. Swanson**[c], **Joseph O. Falkinham III**[d], **Mansukh C. Wani**[e], **Cedric J. Pearce**[f], and **Nicholas H. Oberlies**[a]

Nicholas H. Oberlies: nicholas_oberlies@uncg.edu

[a]Department of Chemistry and Biochemistry, University of North Carolina at Greensboro, Greensboro, NC 27402, United States, Homepage: http://www.uncg.edu/che/Group_Research_Page/NicholasOberlies

[b]Facultad de Química, Universidad Nacional Autónoma de México Mexico DF 04510, Mexico

[c]Department of Medicinal Chemistry and Pharmacognosy University of Illinois at Chicago, Chicago, IL 60612, United States

[d]Department of Biological Sciences, Virginia Polytechnic Institute and State University, Blacksburg, Virginia 24061, United States

[e]Natural Products Laboratory, Research Triangle Institute, Research Triangle Park NC 27709 United States

[f]Mycosynthetix Inc., Hillsborough, NC 27278, United States

Abstract

Sixteen polyketides belonging to diverse structural classes, including monomeric/dimeric tetrahydroxanthones and resorcylic acid lactones, were isolated from an organic extract of a fungal culture *Setophoma terrestris* (MSX45109) using bioactivity-directed fractionation as part of a search for anticancer leads from filamentous fungi. Of these, six were new: penicillixanthone B (**5**), blennolide H (**6**), 11-deoxy blennolide D (**7**), blennolide I (**9**), blennolide J (**10**), and pyrenomycin (**16**). The known compounds were: secalonic acid A (**1**), secalonic acid E (**2**), secalonic acid G (**3**), penicillixanthone A (**4**), paecilin B (**8**), aigialomycin A (**11**), hypothemycin (**12**), dihydrohypothemycin (**13**), pyrenochaetic acid C (**14**), and nidulalin B (**15**). The structures were elucidated using a set of spectroscopic and spectrometric techniques; the absolute configurations of compounds **1**–**10** were determined using ECD spectroscopy combined with time-dependent density functional theory (TDDFT) calculations, while a modified Mosher's ester

Correspondence to: Nicholas H. Oberlies, nicholas_oberlies@uncg.edu.

Supporting Information: Molecular modeling calculations, UPLC chromatograms of compounds **1**–**16**, ^{1}H and ^{13}C NMR spectra for compounds **1**–**16**, key COSY, HMBC, and NOESY correlations of **4**, comparison of the experimental ECD spectra of penicillixanthone A (**4**) and penicillixanthone B (**5**), experimental and calculated ECD spectra for blennolide H (**6**), comparison of the experimental ECD spectra of blennolide I (**9**) and blennolide J (**10**), DFT B3LYP/DGDZVP global minimum energy models, relative Gibbs free energies (ΔG_{rel})^{a} and equilibrium population (p)^{b} values for the most relevant conformations of compounds **4**, **5**, and **7**–**10**, and their correponding enantiomers **4a**, **5a**, and **7a**–**10a**, phylogram of the most likely tree; ECD and optical rotation data, experimental vs. literature, of compounds **1**–**4**, **6**, **8**–**9**, and blennolide G, ^{1}H NMR data for **1**–**3**, NMR data for **4**, and NMR data for **8** and paecilin B.

method was used for compound **16**. The cytotoxic activities of compounds (**1**–**15**) were evaluated using the MDA-MB-435 (melanoma) and SW-620 (colon) cancer cell lines. Compounds **1**, **4**, and **12** were the most potent with IC_{50} values ranging from 0.16 to 2.14 μM. When tested against a panel of bacteria and fungi, compounds **3** and **5** showed promising activity against the Gram-positive bacterium *Micrococcus luteus* with MIC values of 5 and 15 μg/mL, respectively.

Keywords

Cytotoxicity; fungus; secalonic acids; ergochromes; resorcylic acid lactones

Introduction

Structurally diverse cytotoxic secondary metabolites have been isolated and identified from filamentous fungi of the Mycosynthetix library, representing over 55,000 accessions, as part of ongoing bioactivity-directed studies for discovery of anticancer drug leads.[1] The organic extract of a solid phase culture of *Setophoma terrestris* (MSX45109), which was isolated from plant material collected in a mangrove habitat in 1989, showed potent cytotoxic activities against the SW-620 (colon) and MDA-MB-435 (melanoma) cancer cell lines (~91% and 100% inhibition of cell growth when tested at 20 μg/mL, respectively). Of the hundreds of cultures that have been investigated as part of this project, *S. terrestris* was intriguing due to the robust biosynthesis of 16 polyketides (**1**–**16**) of distinct structural classes. Over one third of the isolated compounds were new, while structural revisions and augmentations to the literature were developed for several others.

Compounds **1**–**10** were identified as a series of monomeric/dimeric tetrahydroxanthones, an important class of mycotoxins that are produced by a variety of microorganisms with remarkable biological activities, including antitumor, antibacterial, and anti-HIV.[2] In the current study, a series of new monomeric and homo/hetero dimeric tetrahydroxanthones were identified, thereby expanding the diversity of this class of natural products and updating the literature on structural elucidation and absolute configuration considerations of structurally related compounds. These points are also critical for accurate and comprehensive dereplication studies of fungal metabolites, an area of growing prominence in the field.[1a, 3] Interestingly, a recent and comprehensive study reported a similar series of compounds albeit with opposite absolute configuration.[4]

Compounds **11**–**13** were characterized as a series of structurally related resorcylic acid lactones (RALs), a family of benzannulated macrolides that are produced by a variety of fungi with a wide range of biological activities, including antitumor, antifungal, antibiotic, and antiviral.[5] Compounds **14** and **16**, biogenetically related to RALs, were also isolated and identified.

The absolute configurations of compounds **1**–**10** were determined using time-dependent density functional theory (TDDFT) calculations of ECD spectra, while for **16** a modified Mosher's ester method was used. The dimeric tetrahydroxanthone derivatives **1** and **4**, and the RAL **12**, all showed potent inhibition of MDA-MB-435 and SW-620 cancer cell lines.

Alternatively, compounds **3** and **5** showed promising activity against the Gram-positive bacterium *Micrococcus luteus*.

Results and Discussion

The organic extract of a large-scale solid-substrate fungal culture of *S. terrestris* (MSX45109) showed potent cytotoxic activity against the SW-620 and MDA-MB-435 cancer cell lines, and thus, it was fractionated by silica gel flash chromatography to yield five fractions. The third fraction, which eluted with 10% MeOH/$CHCl_3$, showed potent cytotoxic activity on the two cancer cell lines, and as such, it was purified using reversed-phase preparative and semipreparative HPLC to yield polyketides **1**–**16**. The purity of the isolated compounds was verified using UPLC (Figure S1, Supporting Information).

Monomeric/dimeric tetrahydroxanthones

Compounds **1**–**10** were identified as a series of monomeric (**6**–**8**), homodimeric (**1**–**5**), and heterodimeric (**9** and **10**) tetrahydroxanthones by comparison of HRMS, NMR, and ECD data with each other and with structurally related compounds (Figure 1). Stereoisomeric compounds **1** (35.1 mg), **2** (51.3 mg), and **3** (9.5 mg) were all obtained as yellow powders and had molecular formulae of $C_{32}H_{30}O_{14}$ as determined by HRESIMS. The ^{1}H and ^{13}C NMR spectra of compounds **1** and **2** showed the presence of only 15 protons and 16 carbons, indicating that these compounds were homodimers, whereas **3** was clearly a heterodimer (Figures S2–S4). A search of the "Dictionary of Natural Products"[6] for the molecular formula and a UV range of 325–345 nm resulted in twelve hits, five of which were excluded based on NMR data. The remaining seven hits were the secalonic acids A–G, all of which contained a 2,2′-linkage. The fact that compounds **1** and **2** were homodimeric cut down the number of possibilities for compounds **1** and **2** into secalonic acids A, B, D, or E, while the heterodimeric nature of **3** suggested either secalonic acid C, F, or G. Key differences between compounds **1** and **2** were the chemical shift values and splitting patterns of H-5, H-6, and H_2-7. A proton doublet of doublets corresponding to H-5/H-5′ (δ_H 3.92, dd, J = 11.2, 0.5 Hz) in **1** was downfield shifted in **2** (δ_H 4.11, d, J = 1.2 Hz). These J values implied a pseudodiaxial *trans* orientation of H-5/H-6 in **1** and a pseudoaxial/pseudoequatorial *cis* orientation in **2** (Figures S2 and S3, Table S1). On the other hand, the ^{1}H NMR spectrum of **3** showed similarity with the ^{1}H NMR spectra of both **1** and **2**, revealing two sets of protons corresponding to asymmetric monomers (Figure S4, Table S1). The 2,2′-linkage in **1**–**3** was confirmed by diagnostic HMBC correlations of H-3 and H-3′ with C-2′ and C-2, respectively. The absolute configurations of the 2,2′-secalonic acids have been determined by ECD spectroscopy.[7] The Cotton effect around 330 nm corresponds to the n–π* electronic transition, and it has been correlated with the configurations of C-10a and C-10a′.[7a, 8] Negative Cotton effects at 332 nm in the ECD spectra of compounds **1**, **2**, and **3** ($\Delta\varepsilon$ = −38.8, −24.6, and −31.2, respectively), indicated an *S*-configuration at both C-10a and C-10a′ (Figure 2). This allowed the assignment of the *R*-configuration at C-6 and C-6′ based on the *trans* orientation of C-6/6′ and C-10a/10a′ substituents deduced from the biosynthetic route for the formation of stereoisomeric tetrahydroxanthone precursors of secalonic acids, with no exception so far in literature.[9] Combining all the data together suggested the absolute configuration as (5*S*,6*R*,10a*S*,5′*S*,6′*R*,10a′*S*), (5*R*,6*R*,10a*S*,5′*R*,6′*R*,10a

′*S*), and (5*R*,6*R*,10a*S*,5′*S*,6′*R*,10a′*S*) for compounds **1**–**3**, respectively. Consequently, compounds **1**–**3** were identified as secalonic acid A,[10] secalonic acid E,[11] and secalonic acid G,[12] respectively, in accordance with published data (Table S2). Most literature pertaining to these compounds dates back to the 1960s and 1970s, and therefore, the ^{1}H and ^{13}C NMR data for **1**–**3** were provided in the Supporting Information (Figures S2–S4, Table S1).

Compound **4** (5.4 mg) was obtained as a yellow powder. The chemical formula was determined as $C_{32}H_{30}O_{14}$ by HRESIMS and analysis of ^{1}H, ^{13}C and edited-HSQC NMR data (Figure S5 and Table S3). These data suggested an asymmetric secalonic acid analogue with structural similarity to **1**. However, a key difference between **4** and **1** was the linkage point of the monomeric units, being a 2,2′ in **1** vs. 2,4′ in **4**, which rendered **4** asymmetric, as evidenced by diagnostic HMBC correlations of H-3 and H-3′ with C-4′ and C-4, respectively (Figure S6). The two monomeric moieties in **4** were assigned the same configuration as **1**, as evidenced by a negative Cotton effect at 331 nm in the ECD spectrum of **4** ($\Delta\varepsilon = -24.8$), and negative values of optical rotation for both **1** and **4** (Figures 2 and S7, Table S2). The absolute configuration of **4** was established as (5*S*,6*R*,10a*S*,5′*S*,6′*R*,10a′*S*) by comparing experimental and calculated ECD spectra predicted by the time-dependent density functional theory/electronic circular dichroism (TDDFT-ECD) approach (Figure 3).[13] Briefly, the conformation analysis of the 3D models of compound (5*S*,6*R*,10a*S*,5′*S*, 6′*R*,10a′*S*)-**4** and its hypothetical enantiomer (5*R*,6*S*,10a*R*,5′*R*,6′*S*,10a′*R*)-**4a** gave twelve and eleven conformers, respectively, within a 2 kcal/mol energy window from the global minimum. All conformers were geometrically optimized at the B3LYP/DGDZVP level.[14] Relative free energies (ΔG°) as well as the Boltzmann distribution for the most relevant optimized conformers were given in the supplementary data (Figure S8). The Boltzmann-averaged ECD spectra of re-optimized conformers of **4** using TDDFT showed excellent fit with the experimental data, with a negative Cotton effect around 320 nm (n–π* transition), whereas the **4a** enantiomer showed a positive Cotton effect at the same wavelength (Figure 3). The NMR (Figure S5, Table S3) and optical rotation data (Table S2) were in agreement with those reported for penicillixanthone A, though the absolute configuration was not determined.[15] Interestingly, compound **4** was reported by Kurobane et al.[16] as a chemically rearranged analogue of **1** by dissolving the latter into polar organic solvents, such as pyridine, acetone, and acetonitrile, either at room or higher temperatures for hours to days, depending on the solvent used. This suggests that **4** may have been an artifact of the purification scheme.

Compound **5** (2.1 mg), which was obtained as a yellow powder, had a chemical formula of $C_{32}H_{30}O_{14}$ as determined by HRESIMS and analysis of ^{1}H, ^{13}C and edited-HSQC NMR data (Figure S9), establishing an index of hydrogen deficiency of 18. The NMR data suggested an asymmetric secalonic acid analogue with structural similarity to **2** (Figures 4 and S9, Table 1). However, as was observed in **1** vs. **4**, the 2,2′-linkage in **2** was supplanted by a 2,4′-linkage in **5**, as evidenced by diagnostic HMBC correlations of H-3 and H-3′ with C-4′ and C-4, respectively (Figure 4). Two singlets, corresponding to H-5/H-5′ (δ_H 4.14/3.99) in **5** implied a pseudoaxial/pseudoequatorial *cis* orientation of H-5/H-6 and H-5′/ H-6′, similar to that in **2**, which were further supported by NOESY correlations between

H-5/H-6 and H-5′/H-6′ (Figure 4). The two monomeric moieties in **5** were assigned the same configuration as **2**, as evidenced by a negative Cotton effect at 332 nm in the ECD spectrum of **5**, Δε = −18.9 (Figure S7), and negative values of optical rotation for both compounds (Table S2). The absolute configuration of **5** was established as (5*R*,6*R*,10a*S*,5′*R*,6′*R*,10a′*S*) by comparing experimental and calculated ECD spectra predicted by TDDFT using the same protocol described for compound **4** (Figures 5 and S10).[13a–d] These data suggested the structure of **5**, which was ascribed the trivial name penicillixanthone B. As noted for **4**,[10] compound **5** was potentially an artifact produced by rearrangement of **2** in polar organic solvents.

Compound **6** (0.8 mg) was obtained as a yellow gum. The molecular formula was deduced as $C_{16}H_{16}O_6$ by HRESIMS and analysis of ^1H, ^{13}C and edited-HSQC NMR data (Figure S11), indicating an index of hydrogen deficiency of 9. Inspection of the HRMS and NMR data suggested **6** as a tetrahydroxanthone derivative with structural similarity to the monomeric unit of **1**. However, key differences were the replacement of the C-2 quaternary carbon in **1** (δ_C 118.3) by an aromatic methine in **6** (δ_H/δ_C 6.54/110.5), and the replacement of the hydrogen-bonded phenolic proton in **1** (δ_H 13.78) by an olefinic proton in **6** (δ_H 7.23) (Table 2, Figure S11). COSY data identified two spin systems as H-2/H-3/H-4 and H-5/H-6/H_2-7/H-8 (Figure 4). Further examination of the NMR spectra, including HMBC data (Figure 4), yielded the planar structure of **6**, which was ascribed the trivial name blennolide H. The relative configuration of **6** was found to be (5*S*,6*R*,10a*S*), the same as that of the monomeric units of **1**, deduced from NOESY correlations and coupling constants for both compounds (Figure 4). However, the ECD calculations suggested the opposite configuration (5*R*,6*S*,10a*R*) (Figure S12). Since this finding was inconsistent with biosynthetic considerations, the calculations were repeated yielding identical results. As such, we consider the absolute configuration of **6** as tentative.

Diastereoisomers **7** (5.4 mg) and **8** (1.0 mg) were obtained as colorless oils and both had molecular formulae of $C_{16}H_{16}O_7$, as determined by HRESIMS and analysis of ^1H, ^{13}C and edited-HSQC NMR data (Figures S13 and S14), establishing an index of hydrogen deficiency of 9. Compounds **7** and **8** showed similar ^1H and ^{13}C NMR spectra (Table 3) with small differences in four chemical shift values. Interestingly, compounds **7** and **8** displayed opposite signs for optical rotation data; while compound **7** was levorotatory (−26.14°), compound **8** was dextrorotary (+42.05°) (Table S2). Moreover, the ECD spectra of **7** and **8** were mirror images (Figure 6). Analysis of the HRMS and NMR data indicated **7** and **8** as monomers and structurally related to the monomeric units of compounds **1–5**. In comparison to the chromanone moiety in compounds **1–5**, rings A and B, were preserved in **7** and **8**, as evidenced from comparable ^{13}C NMR data and the hydrogen-bonded phenolic proton (δ_H 11.43), except for a quaternary aromatic carbon that was replaced by an aromatic methine in **7** and **8**. In contrast, however, ring C experienced significant changes, as evidenced from 1D- and 2D-NMR data. For example, the ^{13}C NMR spectra displayed signals characteristic of ester functionalities (δ_C 175.3 and 175.7 for **7** and **8**, respectively; Table 3). Thus, ring C was established as a γ-lactone moiety, as evidenced from the COSY spin system of H-9/H-10/(H_3-13)/H-11 and HMBC correlations from H_3-13 to C-11 and C-9, H-9 to C-12, and H-11 to C-9 (Figure 4). On the other hand, HMBC correlations from

H_2-3 to C-9 and C-14 and from H-9 to C-14 indicated a 2,9-linkage between the chromanone and the γ-lactone moieties, establishing the planar structures of **7** and **8** (Figure 4). The relative configuration of ring C in compounds **7** and **8** was similar based on NOESY correlations between H_3-13 and H-9 and coupling constant values of 4.0 and 3.4 ppm for H-9 in compounds **7** and **8**, respectively, implying a pseudodiaxial *trans* orientation of H-9/H-10 (Figure 4, Table 3). The spatial arrangement of **7** and **8** were different, as observed via NOESY data, particularly between H-10 to H-11α and H-3α, as well as H-9 to H_2-3 in **7** and from H-9 to H-3α in **8** (Figure 4). Putting these data together, and taking into consideration the fact that compounds **7** and **8** could not be enantiomers, since they were separated using non-enantioselective methods, compounds **7** and **8** could either be epimers in C-2 (2*R*9*S*10*S* or 2*S*9*S*10*S*) or have the same configuration at C-2 but the opposite configuration of ring C. The absolute configuration of **7** and **8** was established by comparing the experimental ECD data with those obtained through molecular modeling calculations (Figures S15 and S16). The excellent fit between the observed and calculated ECD plots (Figure 7) established the absolute configuration of **7** as (2*S*,9*S*,10*S*) and for **8** as (2*R*,9*S*,10*S*), supporting epimerization at C-2. The NMR (Table S4) and optical rotation data of **8** (Table S2) indicated similarity with paecilin B, which was isolated from the mangrove endophytic fungus, *Paecilomyces* sp., and its planar structure was published in 2007.[17] However, significant differences in the ^{1}H and ^{13}C NMR data of compound **8** and paecilin B were observed (Table S4). Recently, paecilin B was reported as a monomer and as a subunit of a dimer from the seagrass-derived fungus *Bipolaris* sp.[18] Our data were in agreement with the latter study, including the absolute configuration. With respect to compound **7**, two structurally related compounds, blennolide D and blennolide E, where C-11 is hydroxylated, were reported previously from *Blennoria* sp.[4] Hence, the trivial name 11-deoxyblennolide D was ascribed to **7**. The planar structure of compounds **7** and **8** was reported previously by synthesis but without the reporting of NMR data.[19]

Compound **9** (1.1 mg) was isolated as a yellow gum with a molecular formula of $C_{32}H_{30}O_{14}$ as deduced by HRESIMS, ^{1}H, ^{13}C and edited-HSQC NMR data (Figure S17), indicating an index of hydrogen deficiency of 18. Analysis of the NMR data, including HMBC and NOESY spectra, suggested **9** as a heterodimer, with one monomeric moiety similar to a monomeric unit of **2** and the other similar to **7** (Table 4, 9Figure 4). A key difference between a monomeric moiety in that was related to **7** was replacement of the C-6 aromatic methine (δ_H/δ_C 6.55/110.7) in **7** by a quaternary carbon in **9** ($\delta_{C\text{-}6'}$ 118.1). A 2,6′-linkage in **9** was evident by diagnostic HMBC correlations of H-3 to C-6′ and H-7′ to C-2, respectively, establishing the planar structure of **9** (Figure 4). The absolute configuration was deduced based on the monomeric constituents. The secalonic acid moiety was assigned the same configuration as **2**, evidenced from similar NOESY correlations and coupling constant values of H-5 and preservation of the configuration at C-10a through the series. As well, the moiety similar to **7** was assigned the same configuration as **7** based on consistencies in the ^{1}H, ^{13}C, and NOESY NMR data (Tables 3 and 4, 9Figure 4). Hence, the absolute structure of was assigned as (5*R*,6*R*,10a*S*,2′*S*,9′*S*,10′*S*) and was confirmed by ECD calculations (Figures 8, S18 and S19). The NMR data of **9** were found to be in agreement with those for blennolide G, which was reported previously from *Blennoria* sp.[4] However, compound **9** and blennolide G showed opposite ECD and optical rotation data, and opposite

absolute configuration at four chiral centers, indicating **9** as a diastereoisomer of blennolide G (Table S2, Figure 9). The trivial name blennolide I was ascribed to **9**.

Compound **10** (0.6 mg), which was isolated as a yellow gum, had a molecular formula of $C_{32}H_{30}O_{14}$ as deduced by HRESIMS, ^{1}H, ^{13}C and edited-HSQC NMR data (Figure S20), indicating an index of hydrogen deficiency of 18. Analysis of the NMR data indicated **10** as an asymmetric heterodimer with structural similarity to **9**. Key differences between **9** and **10** were chemical shift values and splitting patterns of H-5, H-6, and H_2-7 (Table 4, Figures S17 and S20). A proton singlet in **9** (δ_H 4.12), corresponding to H-5, was replaced by a doublet of doublets (δ_H 3.93, dd, J = 11.2, 2.7) in **10**, suggesting a pseudodiaxial *trans* orientation of H-5/H-6 in **10**. These data indicated that the secalonic acid moiety in **10** was similar to the monomeric units of **1**, while the 11-deoxyblennolide D moiety was preserved, as in **9**. A 2,6′-linkage in **10**, also similar to **9**, was confirmed by diagnostic HMBC correlations of H-3 with C-6′ and H-7′ with C-2, respectively, establishing the planar structure of **10** (Figure 4). As for **9**, the absolute configuration of **10** was deduced based on the monomeric constituents and ECD calculations as (5*S*,6*R*,10a*S*,2′*S*,9′*S*,10′*S*) (Figures 9, S18 and S21). The trivial name blennolide J was ascribed to compound **10**.

In addition to compounds **1**–**10**, the biogenetically related benzophenone, nidulalin B (**15**, 1.7 mg) was isolated and identified by comparison of its spectroscopic and spectrometric data with those reported in the literature (Figure S26).[20]

Resorcylic acid lactones

Compounds **11**–**13** were identified as the resorcylic acid lactones, aigialomycin A (4.2 mg),[21] hypothemycin (19.6 mg),[22] and dihydrohypothemycin (3.7 mg),[21] respectively (Figures S22–S24), while compound **14** was the biogenetically related pyrenochaetic acid C (2.7 mg) (Figure S25).[23] In all cases, the spectroscopic and spectrometric data were in agreement with those reported in the literature.

Compound **16** (0.8 mg) was isolated as a colorless oil with a molecular formula of $C_{12}H_{14}O_5$ as revealed by HRESIMS, ^{1}H, ^{13}C and edited-HSQC NMR data (Figure S27), indicating an index of hydrogen deficiency of six. UV absorption maxima of 301, 270, and 233 nm were indicative of an aromatic carbonyl compound.[24] Inspection of the NMR data showed signals characteristic of six aromatic carbons, two of which were oxygenated, two doublet aromatic protons with coupling constant values of 2.3 Hz, and two phenolic protons (Table 5, Figure S27). These data suggested a 1,2,3,5-tetrasubstituted benzene ring with two aromatic protons *meta* to each other (Figure S27, Table 5). Benzene ring substituents were confirmed by HMBC correlations (Figure 4). COSY data identified a 1,2,3-trisubtituted pentane moiety (H_2-4/H-3/H-11/H-12/H-13) with C-3 and C-11 being oxygenated and C-4 attached to the benzene ring (Figure 4). HMBC correlations from H_2-4 to C-6 and C-10 confirmed C-5 as the attachment point of the aliphatic side chain with the aromatic ring. Chemical shift values (δ_H/δ_C 4.43/81.1) for H-3/C-3 indicated esterification of C-3 to form a six membered ring with the ester carbonyl (δ_C 170.2) that was attached to the benzene ring at C-2. Further examination of the NMR data yielded the planar dihydroisocoumarin structure of **16**, which was ascribed the trivial name pyrenomycin. The absolute

configuration of **16** was assigned via a modified Mosher's ester method,[25] establishing the configuration as 3*R* and 11*S* (Figure 10). Similar dihydroisocoumarin compounds were isolated previously from marine sponges, plants, fungi, and insects, including hiburipyranone,[26] 3-(2-hydroxypropyl)-8-hydroxy-3,4-dihydroisocoumarin,[27] and (3*S*, 1′*R*)-3-(1-hydroxyethyl)-6,8-dihydroxy-7-methyl-3,4-dihydroisocoumarin.[28]

Cytotoxicity and antimicrobial evaluation of isolated compounds

Compounds (**1**–**15**) were tested for cytotoxicity in the MDA-MB-435 and SW-620 cancer cell lines. Of the tetrahydroxanthone derivatives, **1** and **4** were the most potent with IC_{50} values less than 0.50 μM in both cell lines (Table 6). Based on the cytotoxicity data of related analogues, the importance of the configuration of C-5/C-5′ became evident (Table 6). Compounds **1** and **4**, with 5*S*,5′*S* configuration, were the most potent, with a 2,2′- and a 2,4′-linkages for **1** and **4**, respectively. A 5*S*,5′*R* configuration, as in **3**, was approximately 20 times less active than **1**, while a 5*R*,5′*R* configuration rendered **2** inactive; both had a 2,2′-linkage of the monomeric units. For those with a 2,4′-linkage, compound **5** with 5*R*,5′*R* was approximately 30 times less active than **4**. Heterodimeric **10**, which was composed of the monomeric units of **1** and compound **7**, was approximately 25 times less active than **1**. Compound **9**, which was composed of the monomeric units of **2** and compound **7** was inactive. The difference in the potencies of **10** vs. **9** further supported the importance of the 5*S*,5′*S* configuration, and all three monomeric compounds (**6**–**8**) were inactive. Consistent with the cytotoxicity data obtained in this study, **1** and its chemically rearranged 2,4′-dimer **4** were reported to have equipotent activity against cultured mouse leukemia L1210 cells.[2d] Moreover, **1** has been reported to have a protecting effect of the dopaminergic neurons from 1-methyl-4-phenylpyridinium (MPP+)-induced cell death[29] and to attenuate colchicine-induced apoptosis of the cortical neurons.[30]

In agreement with the literature,[5] cytotoxicity data of the structurally related RALs (**11**–**13**) indicated the importance of the (*Z*)-enone for activity, as in hypothemycin (**12**) (IC_{50} value of 0.58 μM, MDA-MB-435). Alternatively, aigialomycin A (**11**), with an (*E*)-enone, and dihydrohypothemycin (**13**), with a reduced enone, were both inactive (IC_{50} value >10 μM). RALs containing a (*Z*)-enone have been reported as potent inhibitors of several ATPases and kinases, including TAK1.[31]

The antimicrobial activity of the isolated compounds (**1**–**15**) was evaluated against a panel of bacteria and fungi (Tables 7 and S5). Compounds **3** and **5** showed promising activity against the Gram-positive bacterium *Micrococcus luteus* with MIC values of 5 and 15 μg/mL, respectively. Secalonic acid A (**1**) was reported to have activity against *Bacillus subtilis* and *Piriculaia oryzae*[2b] and a phlogistic activity,[32] while penicillixanthone A (**4**) was reported to have medium antibacterial activity against *M. luteus*, *Pseudoalteromonas nigrifaciens*, and *B. subtilis*.[33] Interestingly, compounds **3** and **5**, which were both inactive in cytotoxicity assays, were the most promising in the antimicrobial assays. This finding demonstrates the importance of testing isolated natural compounds in a variety of assays.

Conclusions

A total of 16 polyketides (**1**–**16**), of which six were new, were isolated from a fungal culture of *S. terrestris* (MSX45109). Cytotoxicity assays suggested compounds **1**, **4**, and **12** as the most potent. When evaluated for antimicrobial activity, compounds **3** and **5** showed promising *M. luteus* activity. This fungus was a prolific producer of polyketides, affording the opportunity to examine many analogues in a series of bioassays concomitantly. Moreover, while a few of the known compounds were first described decades ago, this study also served to update the literature with spectroscopic and spectrometric data derived from modern instruments.

Experimental Section

General Procedures

UV and ECD spectra were obtained using a Varian Cary 100 Bio UV-vis spectrophotometer (Varian Inc., Walnut Creek, CA, USA) and an Olis DSM 17 ECD spectrophotometer (Olis, Inc. Bogart, GA, USA), respectively. NMR data were collected using either a JEOL ECA-500 NMR spectrometer operating at 500 MHz for ^{1}H and 125 MHz for ^{13}C, or a JEOL ECS-400 NMR spectrometer operating at 400 MHz for ^{1}H and 100 MHz for ^{13}C and equipped with a high sensitivity JEOL Royal probe and a 24-slot autosampler (both from JEOL Ltd., Tokyo, Japan), or an Agilent 700 MHz NMR spectrometer (Agilent Technologies, Inc., Santa Clara, CA, USA), equipped with a cryoprope, operating at 700 MHz for ^{1}H and 175 MHz for ^{13}C. Residual solvent signals were utilized for referencing. High resolution mass spectra (HRMS) were obtained using a Thermo LTQ Orbitrap XL mass spectrometer equipped with an electrospray ionization source (Thermo Fisher Scientific, San Jose, CA, USA). A Waters Acquity UPLC system (Waters Corp., Milford, MA, USA) utilizing a Waters BEH C_{18} column (1.7 μm; 50 × 2.1 mm) was used to check the purity of the isolated compounds with data collected and analyzed using Empower software. Phenomenex Gemini-NX C_{18} analytical (5 μm; 250 × 4.6 mm), preparative (5 μm; 250 × 21.2 mm), and semipreparative (5 μm; 250 × 10.0 mm) columns (all from Phenomenex, Torrance, CA, USA) were used on a Varian Prostar HPLC system equipped with ProStar 210 pumps and a Prostar 335 photodiode array detector (PDA), with data collected and analyzed using Galaxie Chromatography Workstation software (version 1.9.3.2, Varian Inc.). Flash chromatography was performed on a Teledyne ISCO CombiFlash Rf 200 using Silica Gold columns (both from Teledyne Isco, Lincoln, NE, USA) and monitored by UV and evaporative light-scattering detectors.

Fungal Strain Isolation and Identification

Mycosynthetix fungal strain MSX45109 was isolated from leaf litter collected in a mangrove habitat in 1989. Molecular techniques were used to identify MSX45109 by sequencing the internal transcribed spacer regions 1 & 2 and 5.8S nrDNA (ITS).[34] DNA extraction, PCR amplification, sequencing, and phylogenetic analyses were performed as described previously.[1b, 35] BLAST search in GenBank and the curated BOLD systems (http://www.boldsystems.org/index.php/IDS_OpenIdEngine) database, as well as Q-bank using ITS rDNA sequences suggested that MSX45109 shared high sequence similarity with

several Centraalbureau voor Schimmelcultures (CBS) strains of *Setophoma terrestris* (Pleosporales, Ascomycota) with ≥80% query coverage and 99–100% sequence identity. The top BLAST matches were downloaded using Seaview v4.4.2. and Maximum Likelihood analysis was performed using methods outlined earlier.[36] Based on the results of the BLAST search and Maximum Likelihood phylogeny of the ITS region (Figure S28), the strain MSX45109 was identified as *Setophoma terrestris* (H. N. Hansen) Gorenz J.C. Currently, three species of *Setophoma* have been described with *S. terrestris* as the type species.[37] The ITS sequences of four isolates of MSX45109 were deposited in the GenBank (accession numbers KM203887, KM203888, KM203889, and KM203890).

Fermentation, Extraction and Isolation

Storage, fermentation, and extraction procedures of fungal strain MSX45109 were as described previously.[1b, 1d, 1h] In brief, a seed culture of strain MSX45109 grown in YESD medium was used to inoculate a 2.8-L Fernbach flask (Corning, Inc., Corning, NY, USA) containing 150 g rice and 300 mL H_2O. The solid culture was incubated at r.t. for 14 days and then extracted by addition of a 500 mL mixture of 1:1 MeOH/$CHCl_3$. The culture was chopped into small pieces and left to shake at 125 rpm at r.t., followed by vacuum filtration. The solid phase was washed with 100 mL of 1:1 MeOH/$CHCl_3$. To the filtrate, 900 mL $CHCl_3$ and 1500 mL H_2O were added so that the final ratio of $CHCl_3$/MeOH/H_2O was 4:1:5. The mixture was stirred for ½ h and then transferred into a separatory funnel. The organic bottom layer was drawn off and evaporated to dryness and then re-constituted in 100 mL of 1:1 MeOH/CH_3CN and 100 mL of hexanes. The biphasic solution was stirred for 15 min and then transferred to a separatory funnel. The MeOH/CH_3CN layer was drawn off and evaporated to dryness under vacuum. The defatted material (1.5 g) was dissolved in a mixture of $CHCl_3$/MeOH, adsorbed onto Celite 545, and fractionated via flash chromatography using a gradient solvent system of hexane/$CHCl_3$/MeOH at a 40 mL/min flow rate and 53.3 column volumes over 63.9 min to afford five fractions. Fraction 3 (627 mg) was subjected to preparative reversed phase HPLC over a Phenomenex Gemini-NX C_{18} preparative column using a gradient system of 40:60 to 60:40 over 30 min of CH_3CN/H_2O (acidified with 0.1% formic acid) at a flow rate of 21.24 mL/min to yield thirteen sub-fractions. Sub-fractions 4, 5, 10, and 12 yielded compounds **11** (4.2 mg), **12** (19.6 mg), **1** (35.1), and **2** (48.4 mg), which eluted at 7.8, 8.7, 25.1, and 29.0 min, respectively. The other sub-fractions were subjected to further purifications as follows: sub-fraction 1 (2.3 mg) was subjected to semi-preparative HPLC purification over a Phenomenex Gemini-NX C_{18} column using a gradient system of 50:50 to 70:30 of MeOH/H_2O (0.1% formic acid) over 15 min at a flow rate of 4.72 mL/min to yield compound **16** (0.8 mg), which eluted at 13.1 min. Sub-fraction 6 (8.5 mg) was subjected to preparative HPLC purification using a Phenomenex Gemini-NX C_{18} and a gradient system of 50:50 to 70:30 of MeOH/H_2O (0.1% formic acid) over 15 min at a flow rate of 21.24 mL/min to yield compounds **15** (1.7 mg) and **13** (3.7 mg), which eluted at 8.0 and 18.9 min, respectively. Sub-fraction 7 (1.5 mg) was subjected to semipreparative HPLC purification using a Phenomenex Gemini-NX C_{18} column and a gradient system of 50:50 to 70:30 of MeOH/H_2O (0.1% formic acid) over 15 min at a flow rate of 4.72 mL/min to yield compound **6** (0.8 mg), which eluted at 17.5 min. Sub-fraction 9 (18.2 mg) was subjected to preparative HPLC purification using a Phenomenex Gemini- NX C_{18} and a gradient system of 50:50 to 70:30 of MeOH/H_2O (0.1%

formic acid) over 15 min at a flow rate of 21.24 mL/min to yield compounds **7** (5.4 mg), **8** (1.0 mg), and **14** (2.7 mg), which eluted at 11.6, 13.5 and 19.5 min, respectively. An aliquot of sub-fraction 10 (20 mg) was further purified using preparative HPLC over a Phenomenex Gemini-NX C_{18} utilizing a gradient solvent system of 70:30 to 90:10 of MeOH/H_2O (0.1% formic acid) over 15 min at a flow rate of 21.24 mL/min to yield compounds **10** (0.6 mg) and **1** (3.1 mg), which eluted at 9.5 and 14.8 min, respectively. An aliquot of sub-fraction 11 (20 mg) was subjected to semi-preparative HPLC purification over a Phenomenex Gemini-NX C_{18} column using a gradient system of 70:30 to 90:10 of MeOH/H_2O (0.1% formic acid) over 15 min at a flow rate of 4.72 mL/min to yield compound **3** (9.5 mg), which eluted at 12.3 min, and compound **9** (1.1 mg), which was obtained by yet another round of similar purification. Sub-fraction 13 (21.5 mg) was subjected to preparative HPLC purification using a Phenomenex Gemini-NX C_{18} and a gradient system of 70:30 to 90:10 of MeOH/H_2O (0.1% formic acid) over 15 min at a flow rate of 21.24 mL/min to yield compounds **2** (2.9 mg) and **4** (5.4 mg), which eluted at 10.5 and 19.9 min, respectively, and compound **5** (2.1 mg), which was obtained by another round of HPLC purification.

Penicillixanthone B (5)—Yellow powder; $[\alpha]_D^{20} = -112^\circ$ (*c* = 0.03 in acetone); UV (MeOH) λ_{max} (log ε) 349 (3.64), 336 (3.63), 250 (3.58) nm; CD (*c* 6.26 × 10^{-5} M, $CHCl_3$) λ ($\Delta\varepsilon$) 225 (−55.3) nm, 243 (+48.4) nm, 332 (−18.9) nm; 347 (+2.6) nm, 376 (−8.8) nm; ^{1}H NMR ($CDCl_3$, 500 MHz) and ^{13}C NMR ($CDCl_3$, 125 MHz), see Table 1 and Supplementary Figure S9; HRESIMS *m*/*z* 639.1691 $[M + H]^+$ (calcd for $C_{32}H_{31}O_{14}$ 639.1708).

Blennolide H (6)—Yellow gum; $[\alpha]_D^{20} = -25.3^\circ$ (*c* = 0.01 in chloroform); UV (MeOH) λ_{max} (log ε) 283 (3.48), 193 (3.68) nm; CD (*c* 4.27 × 10^{-4} M, MeOH) λ ($\Delta\varepsilon$) 231 (+11.9) nm, 269 (−20.9) nm, 298 (−19.8) nm; ^{1}H NMR ($CDCl_3$, 500 MHz) and ^{13}C NMR ($CDCl_3$, 175 MHz), see Table 2 and Supplementary Figure S11; HRESIMS *m*/*z* 305.1012 $[M + H]^+$ (calcd for $C_{16}H_{17}O_6$ 305.1020).

11-Deoxyblennolide D (7)—Colorless oil; $[\alpha]_D^{20} = -26.14^\circ$ (c = 0.03 in chloroform); UV (MeOH) λ_{max} (log ε) 349 (3.21), 270 (3.45), 224 (3.37) nm; CD (*c* 1.56 × 10^{-4} M, $CHCl_3$) λ ($\Delta\varepsilon$) 235 (+6.2) nm, 267 (−53.8) nm, 307 (−16.4) nm; 346 (+0.5) nm; ^{1}H NMR ($CDCl_3$, 500 MHz) and ^{13}C NMR ($CDCl_3$, 125 MHz), see Table 3 and Supplementary Figure S13; HRESIMS *m*/*z* 321.0963 $[M + H]^+$ (calcd for $C_{16}H_{17}O_7$ 321.0969).

Paecilin B (8)—Colorless oil; $[\alpha]_D^{20} = +42.05^\circ$ (*c* = 0.09 in chloroform); UV (MeOH) λ_{max} (log ε) 346 (3.20), 271 (3.49), 193 (3.70) nm; CD (*c* 5.62 × 10^{-4} M, $CHCl_3$) λ ($\Delta\varepsilon$) 235 (−44.7) nm, 267 (+35.2) nm, 307 (+17.0) nm; 346 (−8.7) nm; ^{1}H NMR ($CDCl_3$, 500 MHz) and ^{13}C NMR ($CDCl_3$, 125 MHz), see Table 3 and Supplementary Figure S14; HRESIMS *m*/*z* 321.0961 $[M + H]^+$ (calcd for $C_{16}H_{17}O_7$ 321.0969).

Blennolide I (9)—Yellow powder; $[\alpha]_D^{20} = -102.30^\circ$ (*c* = 0.09 in chloroform); UV (MeOH) λ_{max} (log ε) 349 (2.81), 258 (3.69), 224 (3.69) nm; CD (*c* 6.26 × 10^{-5} M, $CHCl_3$) λ ($\Delta\varepsilon$) 241 (+13.9), 275 (−6.3) nm, 334 (−8.7) nm; ^{1}H NMR ($CDCl_3$, 700 MHz) and ^{13}C NMR ($CDCl_3$,

175 MHz), see Table 4 and Supplementary Figure S17; HRESIMS *m*/*z* 639.1682 $[M + H]^+$ (calcd for $C_{32}H_{31}O_{14}$ 639.1708).

Blennolide J (10)—Yellow powder; $[\alpha]_D^{20} = -93.5°$ (*c* = 0.08 in chloroform); UV (MeOH) λ_{max} (log ε) 349 (3.37), 336 (3.37), 237 (3.4) nm; CD (*c* 1.72 × 10^{-4} M, $CHCl_3$) λ ($\Delta\varepsilon$) 245 (+38.9), 262 (−14.9) nm, 337 (−13.9) nm, 377 (−16.7) nm; ^{1}H NMR ($CDCl_3$, 700 MHz) and ^{13}C NMR ($CDCl_3$, 175 MHz), see Table 4 and Supplementary Figure S20; HRESIMS *m*/*z* 639.1683 $[M + H]^+$ (calcd for $C_{32}H_{31}O_{14}$ 639.1708).

Pyrenomycin (16)—Coreless oil; $[\alpha]_D^{20} = -5.7°$ (*c* = 0.05 in chloroform); UV (MeOH) λ_{max} (log ε) 301 (3.09), 270 (3.12), 233 (3.07) nm; ^{1}H NMR (Methnol-d_4, 700 MHz) and ^{13}C NMR (Methnol-d_4, 175 MHz), see Table 5 and Supplementary Figure S27; HRESIMS *m*/*z* 239.0909 $[M + H]^+$ (calcd for $C_{12}H_{16}O_5$ 239.0914).

Preparation of The (*R*)- And (*S*)-MTPA Ester Derivatives of Pyrenomycin (16)

To 0.1 mg of compound **16** were added 400 μL of pyridine-d_5, and the solution was transferred into an NMR tube. To initiate the reaction, 20 μL of *S*-(+)-α-methoxy-α-(trifluoromethyl)phenylacetyl (MTPA) chloride were added with careful shaking and then monitored immediately by ^{1}H NMR at the following time points: 0, 5, 10, 15, 30, 60, and 120 min. The reaction was found to be complete in 2 h, yielding the mono (*R*)-MTPA ester derivative (**16b**) of **16**. ^{1}H NMR data of **16b** (500 MHz, pyridine-d_5): δ_H 1.85 (3H, d, *J* = 7.5, H_3-13), 1.81 (1H, m, H-12a), 1.90 (1H, m, H-12b), 4.81 (1H, m, H-11), 5.61 (1H, m, H-3). In an analogues manner, 0.1 mg of compound **16** dissolved in 400 μL pyridine-d_5 were reacted in a second NMR tube with 20 μL (*R*)-(−)-α-MTPA chloride for 1 h, to afford the mono (*S*)-MTPA ester (1**6a**). ^{1}H NMR data of **16a** (500 MHz, pyridine-d_5): δ_H 1.75 (3H, d, *J* = 6.9, H_3-13), 1.70 (1H, m, H-12a), 1.80 (1H, m, H-12b), 4.85 (1H, m, H-11), 5.65 (1H, m, H-3).

Molecular Modeling Calculations

Theoretical calculations of ECD spectra for compounds **4**, **5** and **7**–**10**, and their corresponding enantiomers or epimers, were performed with the Gaussian 09 (Gaussian Inc., Wallingford CT, USA) program package as described previously[13e] (for detail see Supplementary Information).[38]

Cytotoxicity assay

The cytotoxicity of compounds (**1**–**15**) were tested against the MDA-MB-435[39] human melanoma (HTB-129, ATCC) and the SW-620[40] human colorectal adenocarcinoma (CCL-227, ATCC) cell lines as described previously.[41]

Antimicrobial assay

Minimal inhibitory concentrations (MICs) of compounds (**1**–**15**) were measured against a panel of bacteria and fungi as described previously.[41a] All measurements were made in duplicate.

Supplementary Material

Refer to Web version on PubMed Central for supplementary material.

Acknowledgments

This research was supported by program project grant P01 CA125066 from the National Cancer Institute/National Institutes of Health, Bethesda, MD, USA. The high resolution mass spectrometry data were acquired at the Triad Mass Spectrometry Laboratory at the University of North Carolina at Greensboro. We are indebted to Dirección General de Cómputo y de Tecnologías de Información y Comunicación (DGTIC), UNAM, for providing the resources to carry out computational calculations through the KanBalam system.

References

1. a) El-Elimat T, Figueroa M, Ehrmann BM, Cech NB, Pearce CJ, Oberlies NH. J Nat Prod. 2013; 76:1709–1716. [PubMed: 23947912] b) El-Elimat T, Figueroa M, Raja HA, Graf TN, Adcock AF, Kroll DJ, Day CS, Wani MC, Pearce CJ, Oberlies NH. J Nat Prod. 2013; 76:382–387. [PubMed: 23301853] c) El-Elimat T, Zhang X, Jarjoura D, Moy FJ, Orjala J, Kinghorn AD, Pearce CJ, Oberlies NH. ACS Med Chem Lett. 2012; 3:645–649. [PubMed: 22993669] d) Figueroa M, Graf TN, Ayers S, Adcock AF, Kroll DJ, Yang J, Swanson SM, Munoz-Acuna U, Carcache de Blanco EJ, Agrawal R, Wani MC, Darveaux BA, Pearce CJ, Oberlies NH. J Antibiot. 2012; 65:559–564. [PubMed: 22968289] e) Sy-Cordero AA, Graf TN, Adcock AF, Kroll DJ, Shen Q, Swanson SM, Wani MC, Pearce CJ, Oberlies NH. J Nat Prod. 2011; 74:2137–2142. [PubMed: 21978324] f) Sy-Cordero AA, Pearce CJ, Oberlies NH. J Antibiot. 2012; 65:541–549. [PubMed: 22990381] g) Ayers S, Ehrmann BM, Adcock AF, Kroll DJ, Wani MC, Pearce CJ, Oberlies NH. Tetrahedron Lett. 2011; 52:5733–5735. [PubMed: 22566715] h) Ayers S, Graf TN, Adcock AF, Kroll DJ, Matthew S, Carcache de Blanco EJ, Shen Q, Swanson SM, Wani MC, Pearce CJ, Oberlies NH. J Nat Prod. 2011; 74:1126–1131. [PubMed: 21513293] i) Ayers S, Graf TN, Adcock AF, Kroll DJ, Shen Q, Swanson SM, Matthew S, Carcache de Blanco EJ, Wani MC, Darveaux BA, Pearce CJ, Oberlies NH. J Antibiot. 2012; 65:3–8. [PubMed: 22068158] j) Ayers S, Graf TN, Adcock AF, Kroll DJ, Shen Q, Swanson SM, Wani MC, Darveaux BA, Pearce CJ, Oberlies NH. Tetrahedron Lett. 2011; 52:5128–5230. [PubMed: 22025810]
2. a) Braäse S, Encinas A, Keck J, Nising CF. Chem Rev. 2009; 109:3903–3990. [PubMed: 19534495] b) Masters KS, Bräse S. Chem Rev. 2012; 112:3717–3776. [PubMed: 22617028] c) Stoll A, Renz J, Brack A. Helv Chim Acta. 1952; 35:2022–2034.d) Kurobane I, Iwahashi S, Fukuda A. Drugs Exp Clin Res. 1987; 13:339–344. [PubMed: 3652923] e) Liao G, Zhou J, Wang H, Mao Z, Xiao W, Wang H, She Z, Zhu Y. Oncol Rep. 2010; 23:387–395. [PubMed: 20043099] f) McPhee F, Caldera PS, Bemis GW, McDonagh AF, Kuntz ID, Craik CS. Biochem J. 1996; 320(Pt 2):681–686. [PubMed: 8973584]
3. a) Ito T, Masubuchi M. J Antibiot. 2014; 67:353–360. [PubMed: 24569671] b) Yang JY, Sanchez LM, Rath CM, Liu X, Boudreau PD, Bruns N, Glukhov E, Wodtke A, de Felicio R, Fenner A, Wong WR, Linington RG, Zhang L, Debonsi HM, Gerwick WH, Dorrestein PC. J Nat Prod. 2013; 76:1686–1699. [PubMed: 24025162] c) Klitgaard A, Iversen A, Andersen MR, Larsen TO, Frisvad JC, Nielsen KF. Anal Bioanal Chem. 2014; 406:1933–1943. [PubMed: 24442010]
4. Zhang W, Krohn K, Ullah Z, Florke U, Pescitelli G, Di Bari L, Antus S, Kurtan T, Rheinheimer J, Draeger S, Schulz B. Chem - Eur J. 2008; 14:4913–4923. [PubMed: 18425741]
5. Bräse, S.; Gläser, F.; Kramer, CS. The Chemistry of Mycotoxins. Bräse, S.; Gläser, F.; Kramer, C.; Lindner, S.; Linsenmeier, AM.; Masters, KS.; Meister, AC.; Ruff, BM.; Zhong, S., editors. Springer; Vienna: 2013. p. 91-108.
6. Dictionary of Natural Products Online 23.1. Taylor & Francis Group; London: 2014.
7. a) Andersen R, Buchi G, Kobbe B, Demain AL. J Org Chem. 1977; 42:352–353. [PubMed: 830866] b) Steyn PS. Tetrahedron. 1970; 26:51–57. [PubMed: 5415401]
8. a) Steyn PS. Tetrahedron. 1970; 26:51–57. [PubMed: 5415401] b) Elsässer B, Krohn K, Flörke U, Root N, Aust HJ, Draeger S, Schulz B, Antus S, Kurtán T. Eur J Org Chem. 2005; 2005:4563–4570.

9. Kurobane I, Vining LC, Mcinnes AG. J Antibiot. 1979; 32:1256–1266. [PubMed: 541252]
10. Franck B, Gottschalk EM, Ohnsorge U, Hüper F. Chem Ber. 1966; 99:3842–3862.
11. Howard CC, Johnstone RAW, Entwistle ID. J Chem Soc, Chem Commun. 1973:464–464.
12. Kurobane I, Vining LC, McInnes AG. Tetrahedron Lett. 1978; 19:4633–4636.
13. a) Bringmann G, Bruhn T, Maksimenka K, Hemberger Y. Eur J Org Chem. 2009; 2009:2717–2727.b) Stephens PJ, Harada N. Chirality. 2010; 22:229–233. [PubMed: 19408332] c) Stephens PJ, Pan JJ, Devlin FJ, Urbanová M, Hájícček J. J Org Chem. 2007; 72:2508–2524. [PubMed: 17338574] d) Acunña UM, Figueroa M, Kavalier A, Jancovski N, Basile MJ, Kennelly EJ. J Nat Prod. 2010; 73:1775–1779. [PubMed: 21028890] e) El-Elimat T, Raja HA, Figueroa M, Falkinham JO III, Oberlies NH. Phytochemistry. 2014; 104:114–120. [PubMed: 24833033] f) Ding Y, Li XC, Ferreira D. J Nat Prod. 2008; 72:327–335. [PubMed: 19099470]
14. a) Godbout N, Salahub DR, Andzelm J, Wimmer E. Can J Chem. 1992; 70:560–571.b) Andzelm J, Wimmer E. The Journal of Chemical Physics. 1992; 96:1280–1303.
15. Jiang T, Tian L, Guo AH, Fu HZ, Pei YH, Lin WH. Acta Pharm Sin. 2002; 37:271–274.
16. Kurobane, I.; Vining, LC.; Mcinnes, AG. U. S. Patent. Asahi Kasei Kogyo Kabushiki Kaisha; Osaka, Japan: 1984. p. 1-9.
17. Guo ZY, She ZG, Shao CL, Wen L, Liu F, Zheng ZH, Lin YC. Magn Reson Chem. 2007; 45:777–780. [PubMed: 17619228]
18. Arunpanichlert J, Rukachaisirikul V, Tadpetch K, Phongpaichit S, Hutadilok-Towatana N, Supaphon O, Sakayaroj J. Phytochem Lett. 2012; 5:604–608.
19. Bose NK, Chaudhury DN. J Indian Chem Soc. 1966; 43:411–415.
20. Kawahara N, Sekita S, Satake M, Udagawa S, Kawai K. Chem Pharm Bull. 1994; 42:1720–1723.
21. Isaka M, Suyarnsestakorn C, Tanticharoen M, Kongsaeree P, Thebtaranonth Y. J Org Chem. 2002; 67:1561–1566. [PubMed: 11871887]
22. Agatsuma T, Takahashi A, Kabuto C, Nozoe S. Chem Pharm Bull. 1993; 41:373–375.
23. Sato H, Konoma K, Sakamura S. Agric Biol Chem. 1981; 45:1675–1679.
24. Pretsch, E.; Bühlmann, P.; Affolter, C. Structure Determination of Organic Compounds: Tables of Spectral Data. Springer; 2000.
25. Hoye TR, Jeffrey CS, Shao F. Nat Protoc. 2007; 2:2451–2458. [PubMed: 17947986]
26. Fusetani N, Sugawara T, Matsunaga S, Hirota H. J Org Chem. 1991; 56:4971–4974.
27. Gao G, Qi S, Zhang S, Yin H, Xiao Z, Li M, Li Q. Pharmazie. 2008; 63:542–544. [PubMed: 18717492]
28. Jiang HL, Luo XH, Wang XZ, Yang JL, Yao XJ, Crews P, Valeriote FA, Wu QX. Fitoterapia. 2012; 83:1275–1280. [PubMed: 22735600]
29. Zhai A, Zhu X, Wang X, Chen R, Wang H. Eur J Pharmacol. 2013; 713:58–67. [PubMed: 23665112]
30. Zhai A, Zhang Y, Zhu X, Liang J, Wang X, Lin Y, Chen R. Neurochem Int. 2011; 58:85–91. [PubMed: 21073911]
31. a) Serba C, Winssinger N. Eur J Org Chem. 2013; 2013:4195–4214.b) Wu JQ, Powell F, Larsen NA, Lai ZW, Byth KF, Read J, Gu RF, Roth M, Toader D, Saeh JC, Chen HW. ACS Chem Biol. 2013; 8:643–650. [PubMed: 23272696]
32. Harada M, Yano S, Watanabe H, Yamazaki M, Miyaki K. Chem Pharm Bull. 1974; 22:1600–1606. [PubMed: 4434583]
33. Bao J, Sun YL, Zhang XY, Han Z, Gao HC, He F, Qian PY, Qi SH. J Antibiot. 2013; 66:219–223. [PubMed: 23232928]
34. Schoch CL, Seifert KA, Huhndorf S, Robert V, Spouge JL, Levesque CA, Chen W. Fungal Barcoding Consortium. Proc Natl Acad Sci USA. 2012; 109:6241–6246. [PubMed: 22454494]
35. a) El-Elimat T, Figueroa M, Raja HA, Adcock AF, Kroll DJ, Swanson SM, Wani MC, Pearce CJ, Oberlies NH. Tetrahedron Lett. 2013; 54:4300–4302. [PubMed: 23956472] b) Figueroa M, Raja H, Falkinham JO, Adcock AF, Kroll DJ, Wani MC, Pearce CJ, Oberlies NH. J Nat Prod. 2013; 76:1007–1015. [PubMed: 23806109] c) Raja HA, Oberlies NH, El-Elimat T, Miller AN, Zelski SE, Shearer CA. Mycoscience. 2013; 54:353–361.d) Raja HA, Oberlies NH, Figueroa M, Tanaka

K, Hirayama K, Hashimoto A, Miller AN, Zelski SE, Shearer CA. Mycologia. 2013; 105:959–976. [PubMed: 23709484]

36. a) El-Elimat T, Raja HA, Graf TN, Faeth SH, Cech NB, Oberlies NH. J Nat Prod. 2014; 77:193–199. [PubMed: 24456525] b) Figueroa M, Jarmusch AK, Raja HA, El-Elimat T, Kavanaugh JS, Horswill AR, Cooks RG, Cech NB, Oberlies NH. J Nat Prod. 2014; 77:1351–1358. [PubMed: 24911880]
37. a) de Gruyter J, Woudenberg JH, Aveskamp MM, Verkley GJ, Groenewald JZ, Crous PW. Mycologia. 2010; 102:1066–1081. [PubMed: 20943506] b) Quaedvlieg W, Verkley GJ, Shin HD, Barreto RW, Alfenas AC, Swart WJ, Groenewald JZ, Crous PW. Stud Mycol. 2013; 75:307–390. [PubMed: 24014902]
38. Frisch, MJTGW.; Schlegel, HB.; Scuseria, GE.; Robb, MA.; Cheeseman, JR.; Zakrzewski, VG.; Montgomery, JA., Jr; Vreven, T.; Kudin, KN.; Burant, JC.; Millam, JM.; Iyengar, SS.; Tomasi, J.; Barone, V.; Mennucci, B.; Cossi, M.; Scalmani, G.; Rega, N.; Petersson, GA.; Nakatsuji, H.; Hada, M.; Ehara, M.; Toyota, KFR.; Hasegawa, J.; Ishida, MNT.; Honda, Y.; Kitao, O.; Nakai, H.; Klene, M.; Li, X.; Knox, JE.; Hratchian, HP.; Cross, JB.; Adamo, C.; Jaramillo, J.; Gomperts, R.; Stratmann, RE.; Yazyev, O.; Austin, AJ.; Cammi, R.; Pomelli, C.; Ochterski, JW.; Ayala, PY.; Morokuma, K.; Voth, GA.; Salvador, P.; Dannenberg, JJ.; Zakrzewski, VG.; Dapprich, S.; Daniels, AD.; Strain, MC.; Farkas, O.; Malick, DK.; Rabuck, AD.; Raghavachari, K.; Foresman, JB.; Ortiz, JV.; Cui, Q.; Baboul, AG.; Clifford, S.; Cioslowski, J.; Stefanov, BB.; Liu, G.; Liashenko, A.; Piskorz, P.; Komaromi, I.; Martin, RL.; Fox, DJ.; Keith, T.; Al-Laham, MA.; Peng, CY.; Nanayakkara, A.; Challacombe, M.; Gill, PMW.; Johnson, B.; Chen, W.; Wong, MW.; Gonzalez, C.; Pople, JA. Gaussian 03, ReVision B.02. Gaussian Inc; Pittsburgh, PA: 2003.
39. Rae J, Creighton C, Meck J, Haddad B, Johnson M. Breast Cancer Res Treat. 2007; 104:13–19. [PubMed: 17004106]
40. Leibovitz A, Stinson JC, McCombs WB, McCoy CE, Mazur KC, Mabry ND. Cancer Res. 1976; 36:4562–4569. [PubMed: 1000501]
41. a) El-Elimat T, Figueroa M, Raja HA, Swanson SM, Falkinham JO, Lucas DM, Grever MR, Wani MC, Pearce CJ, Oberlies NH. J Antibiot. 2014 In Press. 10.1038/ja.2014.1125b) El-Elimat T, Raja HA, Falkinham JO, Day CS, Oberlies NH. J Nat Prod. 2014 In Press. 10.1021/np500497r

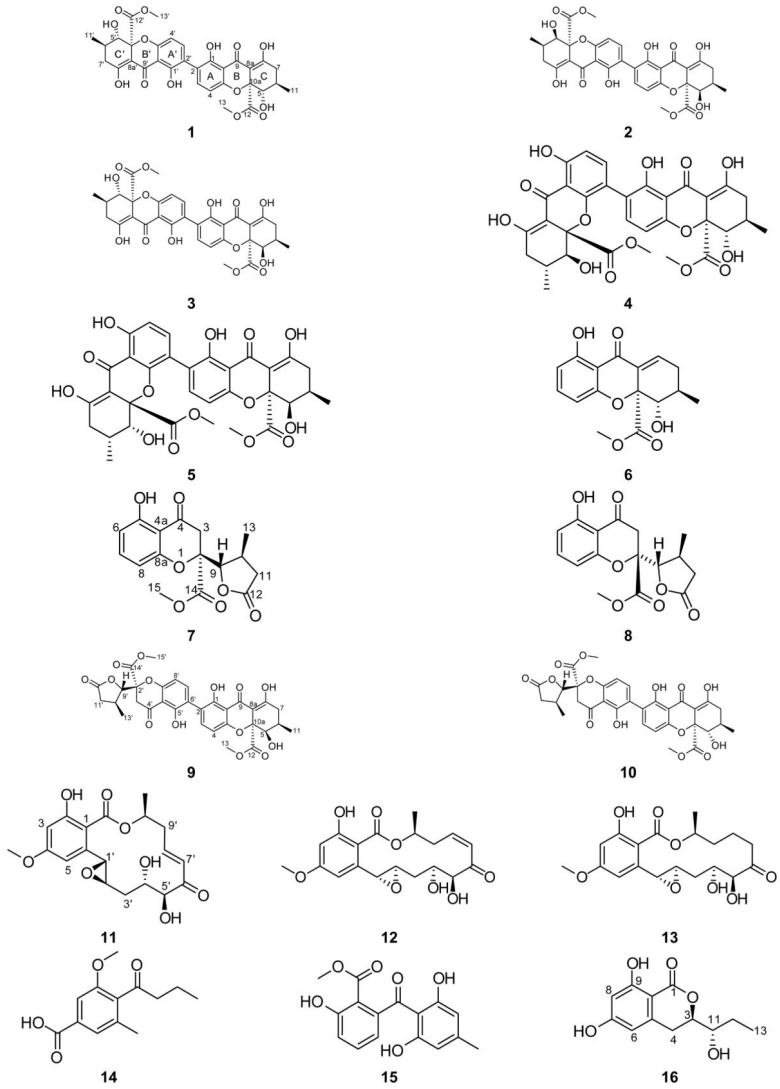

Figure 1.
Compounds **1**–**16** from *S. terrestris* (MSX45109).

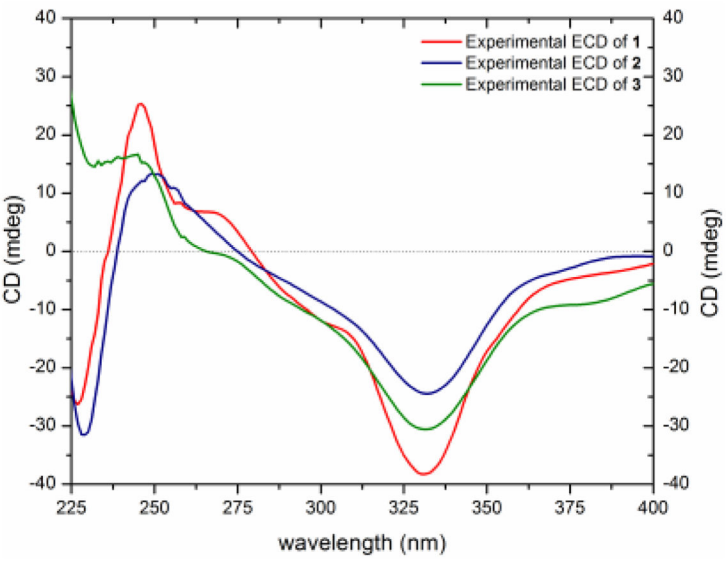

Figure 2.

Comparison of the experimental ECD spectra of secalonic acids A (**1**), E (**2**), and G (**3**) [0.03 mM $CHCl_3$, cell length 2 cm].

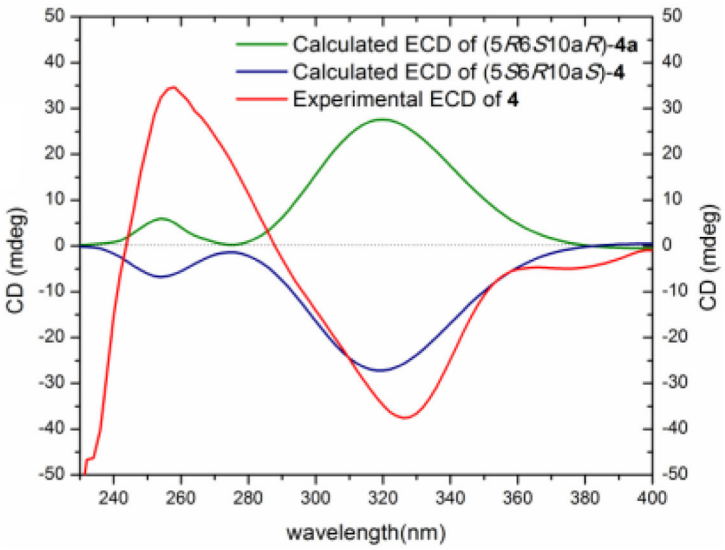

Figure 3.

Experimental and calculated ECD spectra for penicillixanthone A (**4**) [0.05 mM, $CHCl_3$, cell length 2 cm].

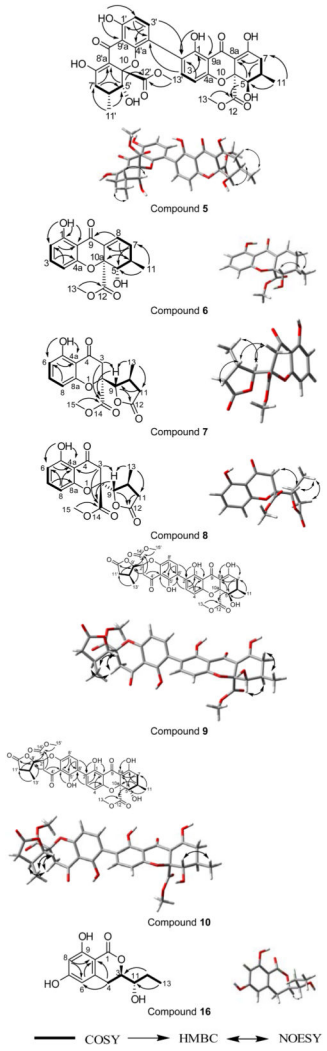

Figure 4.

Key COSY, HMBC, and NOESY correlations of **5–10** and **16**. Based on the NOESY correlations, Gaussian 09 was used for ground state mechanics optimization to generate the structures shown on the right.

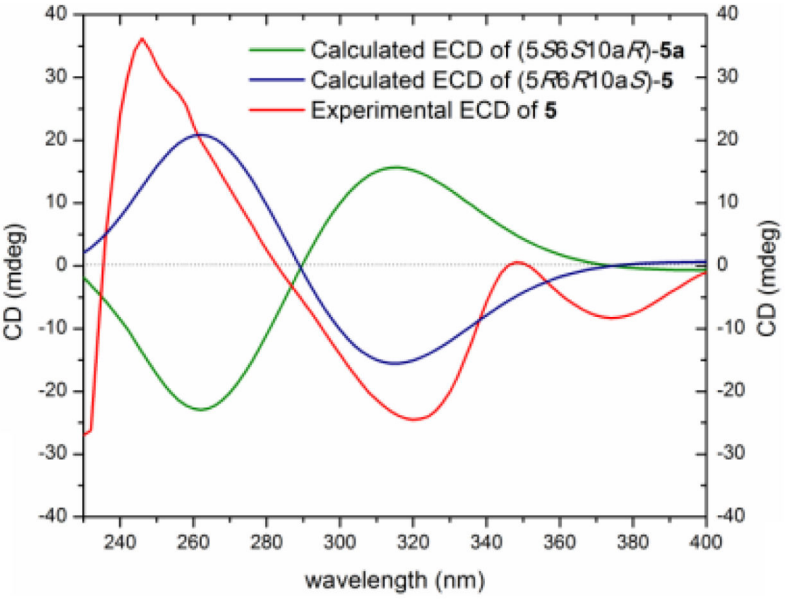

Figure 5.

Experimental and calculated ECD spectra for penicillixanthone B (**5**) [0.06 mM, $CHCl_3$, cell length 2 cm].

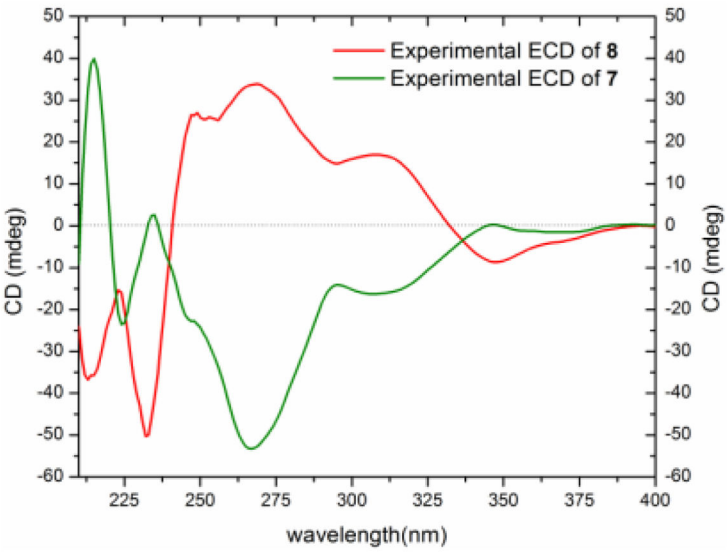

Figure 6.

Experimental ECD spectra of 11-deoxyblennolide D (**7**) [0.16 mM] and paecilin B (**8**) [0.56 mM, $CHCl_3$, cell length 2 cm].

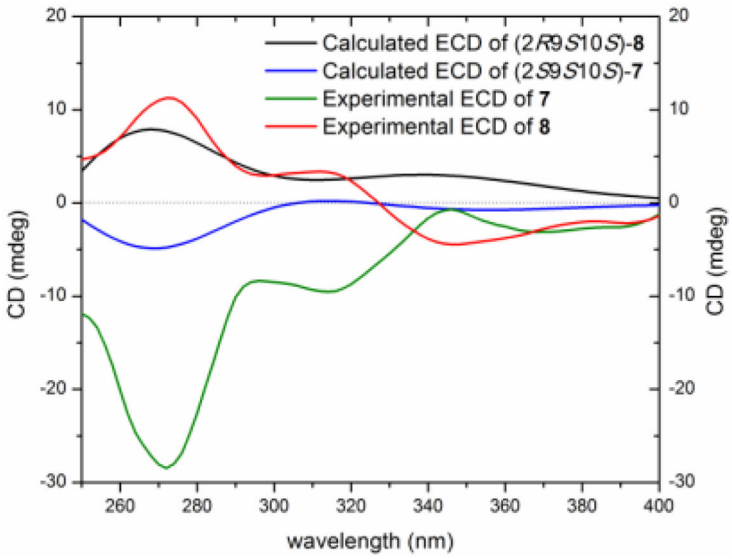

Figure 7.

Experimental and calculated ECD spectra for 11-deoxyblennolide D (**7**) [0.16 mM] and paecilin B (**8**) [0.56 mM, $CHCl_3$, cell length 2 cm].

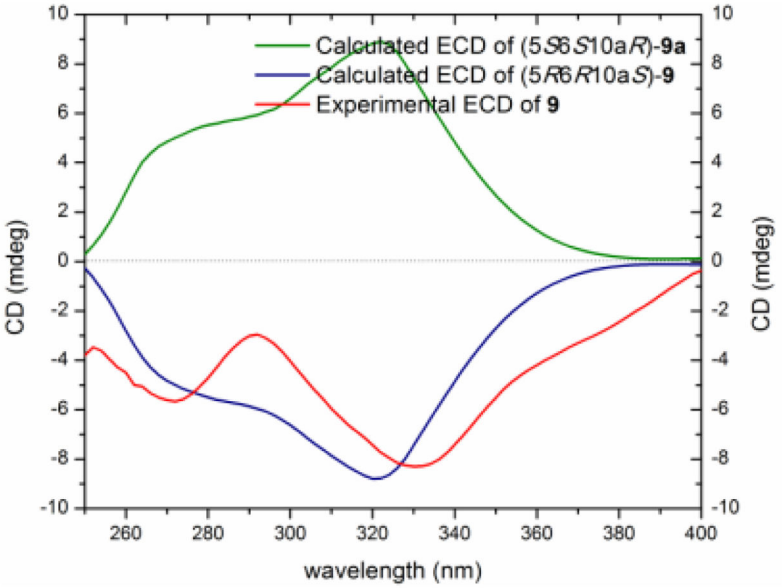

Figure 8.

Experimental and calculated ECD spectra for blennolide I (**9**) [0.06 mM, $CHCl_3$, cell length 2 cm].

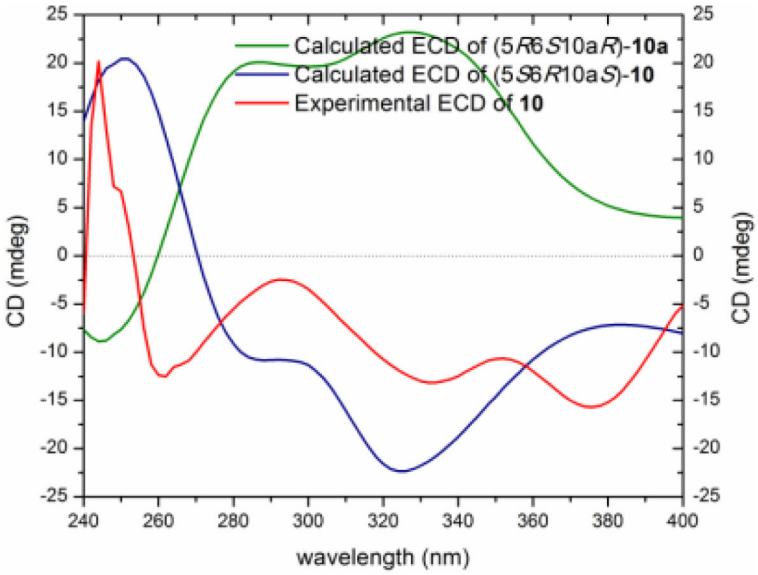

Figure 9.

Experimental and calculated ECD spectra for blennolide J (**10**) [0.17 mM, $CHCl_3$, cell length 2 cm].

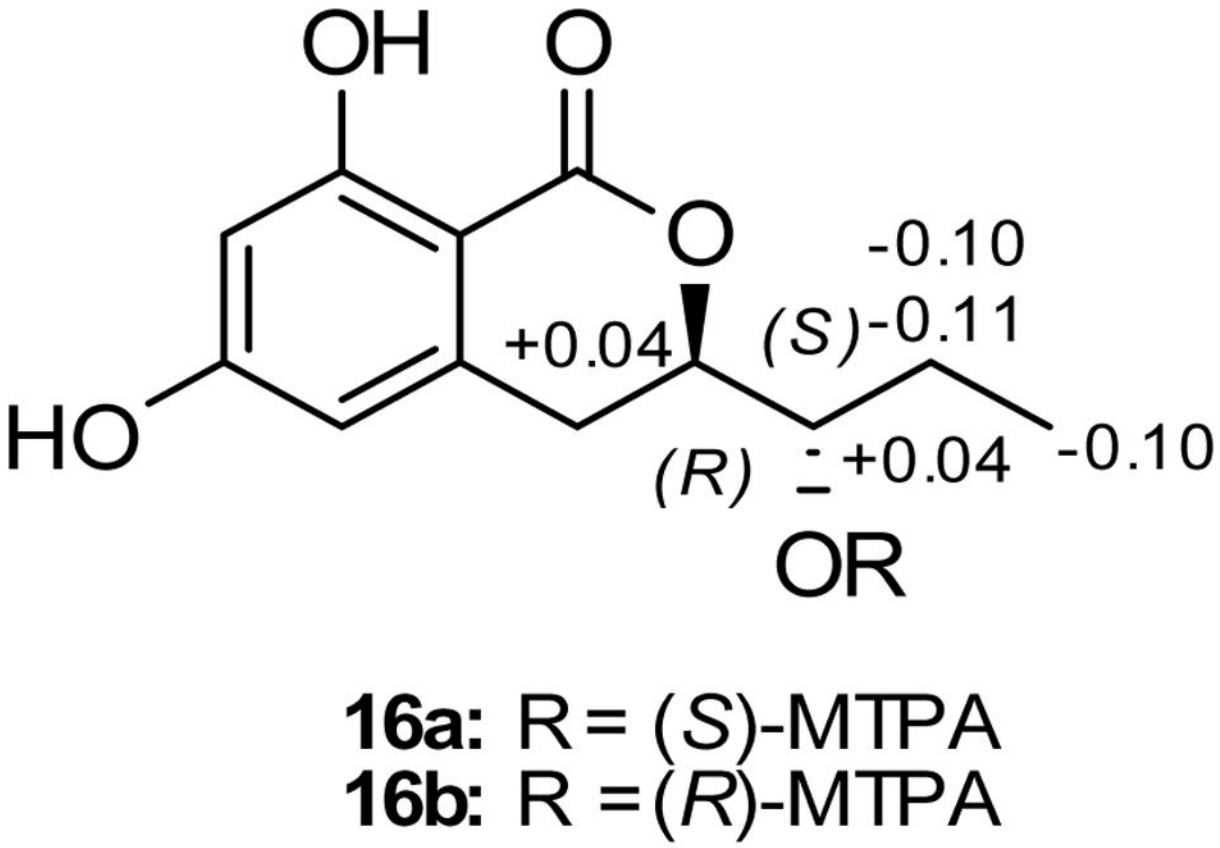

Figure 10.

$\Delta\delta_H$ values [$\Delta\delta$ (in ppm) = $\delta_S - \delta_R$] obtained for (*S*)- and (*R*)-MTPA esters (**16a** and **16b**, respectively) of pyrenomycin (**16**) in pyridine-d_5.

Table 1

NMR data for **5** (500 MHz for ^{1}H, 125 MHz for ^{13}C; chemical shifts in δ, coupling constants in Hz, $CDCl_3$).

Position	δ_C	δ_H mult (*J* in Hz)	Position	δ_C	δ_H mult (*J* in Hz)
1	159.4		1′	161.9	
2	119.4		2′	110.8	6.60, d (8.6)
3	139.6	7.47, d (8.6)	3′	140.1	7.33, d (8.6)
4	107.9	6.58, d (8.6)	4′	115.9	
4a	157.2		4a′	154.5	
5	71.5	4.14, s	5′	70.9	3.99, s
6	28.6	2.12, m	6′	28.5	2.12, m
7	32.7	2.38, m	7′	32.6	2.38, m
		2.49, m			2.49, m
8	180.2		8′	179.4	
8a	99.9		8a′	99.7	
9	187.6		9′	187.9	
9a	107.0		9a′	106.9	
10a	84.9		10a′	84.4	
11	17.6	1.17, dd (6.9, 0.6)	11′	17.6	1.13, dd (6.9, 0.6)
12	171.4		12′	170.9	
13	53.7	3.75, s	13′	53.4	3.64, s
1-OH		11.91, s	1′-OH		11.56, s
5-OH		2.55, brs	5′-OH		2.77, brs

Table 2

NMR data for **6** (500 MHz for ^{1}H, 175 MHz for ^{13}C; chemical shifts in δ, coupling constants in Hz, $CDCl_3$).

Position	δ_C	δ_H mult (*J* in Hz)
1	163.0	
2	110.5	6.54, dd (8.6, 0.6)
3	138.5	7.39, dd (8.6, 8.0)
4	107.7	6.56, dd (8.0, 0.6)
4a	159.5	
5	77.5	3.92, dd (11.5, 2.9)
6	30.0	2.36, m
7	33.8	2.16, ddd (20.6, 10.3, 2.9)
		2.72, dt (20.6, 5.2)
8	141.9	7.23, dd (5.2, 2.9)
8a	129.9	
9	184.7	
9a	107.7	
10a	85.8	
11	17.7	1.15, d (6.3)
12	169.1	
13	53.3	3.69, s
1-OH		12.00, s
5-OH		2.74, s

Table 3

NMR data for **7** and **8** (500 MHz for ^{1}H, 125 MHz for ^{13}C; chemical shifts in δ, coupling constants in Hz, $CDCl_3$).

Position	7		8	
	δ_C	δ_H mult (*J* in Hz)	δ_C	δ_H mult (*J* in Hz)
2	84.3		84.3	
3	39.8	3.04, dd (17.2, 0.6)	40.7	3.07, d (17.2)
		3.17, d (17.2)		3.48, d (17.2)
4	194.1		194.9	
4a	107.7		107.5	
5	162.0		161.9	
6	110.7	6.55, dd (8.6, 0.6)	110.6	6.54, dd (8.6, 0.6)
7	139.2	7.42, t (8.6)	139.0	7.40, t (8.6)
8	107.7	6.54, dd (8.6, 0.6)	107.5	6.49, dd (8.6, 0.6)
8a	159.2		159.3	
9	87.6	4.43, dd (4.0, 0.6)	86.5	4.36, dd (3.4, 0.6)
10	30.1	2.83, m	29.7	2.85, m
11	36.2	2.21, dd (17.8, 4.6)	36.4	2.21, dd (17.8, 4.6)
		2.89, dd (17.8, 9.2)		3.01, dd (17.8, 9.2)
12	175.3		175.7	
13	20.9	1.28, d (6.9)	20.7	1.18, d (6.9)
14	168.9		169.2	
15	53.8	3.72, s	53.7	3.74, s
5-OH		11.43, s		11.45, s

Table 4

NMR data for **9** and **10** (700 MHz for ^{1}H, 175 MHz for ^{13}C; chemical shifts in δ, coupling constants in Hz, $CDCl_3$).

Position	9		10	
	δ_C	δ_H mult (*J* in Hz)	δ_C	δ_H mult (*J* in Hz)
1	159.4		159.3	
2	118.3		117.8	
3	139.6	7.42, d (8.3)	140.1	7.45, d (8.5)
4	107.5	6.57, d (8.3)	107.5	6.62, d (8.5)
4a	157.2		158.4	
5	71.3	4.12, s	78.0	3.93, dd (11.2, 2.7)
6	28.5	2.11, m	29.2	2.41, m
7	32.6	2.40, dd (18.9, 6.1)	36.2	2.32, dd (19.4, 10.6)
		2.52, dd (18.9, 11.2)		2.73, dd (19.4, 6.5)
8	179.9		177.6	
8a	99.9		101.5	
9	187.5		187.1	
9a	107.0		106.9	
10a	84.8		84.8	
11	17.5	1.17, d, (7.1)	18.0	1.17, d, (6.5)
12	171.2		170.2	
13	53.5	3.71, s	53.3	3.71, s
1-OH		11.85, s		11.72, s
5-OH		2.52, brs		2.77, d (2.7)
8-OH		13.95, s		13.76, s
2′	84.2		84.2	
3′	39.7	3.05, d (17.0)	39.7	3.05, d (17.0)
		3.21, d (17.0)		3.21, d (17.0)
4′	194.0		194.0	
4a′	107.6		107.6	
5′	159.2		159.2	
6′	118.1		118.1	
7′	141.3	7.52, d (8.3)	141.3	7.51, d (8.5)
8′	107.3	6.61, d (8.3)	107.3	6.62, d (8.5)
8a′	158.6		158.6	
9′	87.5	4.45, d (3.8)	87.5	4.46, d (4.1)
10′	30.0	2.84, m	30.0	2.84, m
11′	36.0	2.91, dd (18.0, 9.3)	36.0	2.92, dd (17.9, 9.4)
		2.23, dd (18.0, 4.8)		2.22, dd (17.9, 4.6)
12′	175.1		175.1	
13′	20.9	1.28, d (7.1)	20.9	1.28, d (6.8)
14′	168.8		168.8	

Position	9		10	
	δ_C	δ_H mult (*J* in Hz)	δ_C	δ_H mult (*J* in Hz)
15′	53.7	3.76, s	53.7	3.75, s
5′-OH		11.88, s		11.89, s

Table 5

NMR data for **16** (700 MHz for ^{1}H, 175 MHz for ^{13}C; chemical shifts in δ, coupling constants in Hz, Methanol-d_4)

Position	δ_C	δ_H mult (*J* in Hz)
1	170.2	
3	81.1	4.43, dt (12.7, 3.3)
4	29.0	2.75, dd (16.4, 3.3)
		3.11, dd (16.4, 12.7)
5	142.2	
6	107.2	6.21, brd (2.3)
7	164.2	
8	100.9	6.15, d (2.3)
9	168.8	
10	99.6	
11	73.1	3.58, dt (8.6, 3.3)
12	25.1	1.67, m
13	9.2	1.03, t (7.5)
9-OH		8.55, s
11-OH		1.28, brs
7-OH		4.57, brs

Table 6

Cytotoxicity of compounds **1**–**15** against two human tumor cell lines.

Compound[a]	IC_{50} values in μM[b]	
	MDA-MB-435[c]	SW-620[c]
1	0.16	0.41
2	NA	19.12
3	3.27	3.67
4	0.18	0.21
5	5.20	5.55
10	4.06	6.14
12	0.58	2.14

[a] Compounds **6**–**9**, **11**, and **13**–**15** were inactive with IC_{50} values >20 μM.

[b] IC_{50} values were determined as the concentration required to inhibit growth to 50% of control with 72 h incubation.

[c] Positive control was vinblastine tested at concentration of 1 nM in MDA-MB-435 cells and 10 nM in SW620 cells, which had 23% and 76% viable cells, respectively.

Table 7

Antimicrobial activities of compounds **1**–**15**

Compound[a]	Antimicrobial Activity MIC (μg/mL)	
	M. luteus	*S. aureus*
1	38	75
2	36	NA[b]
3	5	39
4	46	93
5	15	59
10	43	43
Vancomycin[c]	--	0.25

[a] See table S5 for compounds **6**–**9**, **11**, and **12**–**15**.

[b] NA: not active with MIC >145 μg/mL.

[c] Positive control..